ChemPubSoc Europe

DOI: 10.1002/cbic.201500641

CHEMBIOCHEM Full Papers

SPECIAL ISSUE

TP-2Rho Is a Sensitive Solvatochromic Red-Shifted Probe for Monitoring the Interactions between CDK4 and Cyclin D

Morgan Pellerano[+],[a] Delphine Naud-Martin[+],[b, c] Marion Peyressatre,[a] Camille Prével,[a] Marie-Paule Teulade-Fichou,[b, c] May Morris,*[a] and Florence Mahuteau-Betzer*[b, c]

Understanding the intricate steps of protein kinase regulation requires characterization of protein–protein interactions between the catalytic subunit, its regulatory partners and the substrate. Fluorescent probes are useful tools with which to study such interactions and to gain insight into their affinities and specificities. Solvatochromic probes, which display changes in their fluorescence emission in response to changes in the polarity of the medium, are particularly attractive. Here we describe conjugation of a switchable fluorescent dye, TP-2Rho, to peptide and protein derivatives of cyclin-dependent kinase 4 (CDK4) and its application to characterization of the interactions between the catalytic subunit of this kinase, its regulatory partner cyclin D1 and a peptide substrate. We demonstrate the sensitivity of TP-2Rho in relation to of those other dyes used for monitoring peptide–protein and protein–protein interactions. Moreover, we show that TP-Rho-labelled peptides can be introduced into living cells to probe endogenous CDK4/cyclin D.

Introduction

Monitoring of protein–protein and peptide–peptide interactions is one of the many approaches that contributes to characterization of the functions and regulation of protein partners in biological signalling pathways. Acquisition of insight into the mechanisms of binding and determination of dissociation constants between protein subunits, enzymes and their substrates, agonists or antagonists are essential to complement structural studies. Likewise, development of new inhibitors for therapeutic means requires determination of their binding sites and affinities for their targets, as well as the characterization of their specificity and selectivity profiles through complementary biochemical, biophysical and biological approaches.

Fluorescent probes are very useful tools with which to study protein and peptide interactions. A wide variety of fluorescent probes with distinctive biophysical properties that might make them more suitable for in vitro or in vivo applications are available.[1] The emission properties of these solvatochromic probes are modified upon modification of the polarity of the medium. Among them, light-up probes have attracted considerable attention. These dyes are not fluorescent in their free forms but become fluorescent when bound to their targets. Their on/off behaviour provides better contrast and therefore better sensitivity to environmental changes.[2] For biological applications, an ideal light-up probe requires additional photophysical and physicochemical properties such as water solubility, red emission and brightness, and there is still an important need for bright and red-emitting dyes.[3]

Recently we have developed a new family of vinyltriphenylamine dyes and shown that the switchable dyes of this class are highly sensitive fluorescent probes for probing DNA by cellular imaging.[4] By changing their acceptor moieties from cationic to anionic variants, with the aim of labelling proteins rather than DNA, we synthesized the TP-Rho class of dyes.[5] These retain the lighting-up properties of the cationic dyes, displaying very efficient fluorescence enhancement ($F/F_0 \approx 80$ for TP-2Rho) when complexed with human serum albumin (used as a model protein).[5] Moreover, the two-photon absorption abilities of TP-Rho dyes, as well as their emission properties ($\lambda_{abs} \approx 600$ nm), are an asset for live-cell imaging. Indeed, infrared excitation causes less damage to the sample than UV/Vis and avoids cellular endogenous fluorescence.[6] These water-soluble and cell-permeant π-conjugated molecules display optical properties that make them attractive candidates for protein- and peptide-based applications.

Cyclin-dependent kinases (CDKs) form a family of heterodimeric kinases that are central to regulation of cell cycle progression, but also play major roles in a wide variety of biologi-

[a] M. Pellerano,[+] M. Peyressatre, Dr. C. Prével, Dr. M. Morris
Institut des Biomolécules Max Mousseron–IBMM-CNRS-UMR 5247
Faculté de Pharmacie, Université Montpellier 1
15, avenue Charles Flahault, 34093 Montpellier (France)
E-mail: may.morris@univ-montp1.fr

[b] D. Naud-Martin,[+] Dr. M.-P. Teulade-Fichou, Dr. F. Mahuteau-Betzer
Institut Curie, PSL Research University
CNRS, INSERM, UMR9187-U1196
91405 Orsay (France)
E-mail: florence.mahuteau@curie.fr

[c] D. Naud-Martin,[+] Dr. M.-P. Teulade-Fichou, Dr. F. Mahuteau-Betzer
Université Paris Sud
Université Paris-Saclay, CNRS, UMR9187-U1196
91405 Orsay (France)

[+] These authors contributed equally to this work.

Supporting information for this article can be found under http://dx.doi.org/10.1002/cbic.201500641.

This article is part of a joint Special Issue between *ChemBioChem* and *ChemMedChem* on Protein–Protein Interactions

cal functions, including transcriptional regulation, neurological functions and metabolism.[7] Moreover, these kinases are targets of interest for cancer therapeutics because their hyperactivation, contributing to sustain uncontrolled cell proliferation, has been documented in a wide variety of cancers.[8] Sequential activation of these kinases throughout the cell cycle is subject to several levels of control, which have been investigated through complementary biological, biochemical, biophysical and structural studies.[9] The assembly between CDKs and cyclins, initially investigated between CDK2 and cyclin A, was shown to involve contacts between both the N-terminal and the C-terminal lobes of CDK2 and cyclin A. This process was described as two-step mechanism that first involves a high-affinity interaction between the C helix of the CDK and the α5 helix of the cyclin, thereby inducing a rotation of the N-terminal lobe of the CDK and consequent alignment of the ATP binding site with the catalytic cleft, followed by conformational reorganization of the C lobe and in particular a positional shift of the CDK activation loop, thereby favouring substrate binding.[9d,h,10] Although this interaction has been extensively studied in the case of CDK2 and cyclin A, there are very few studies relating to the biochemistry of interactions between CDK4 and cyclin D.

This heterodimeric kinase is a key regulator of the G1 phase, integrating mitogenic signals through the Ras signalling pathway to induce exit from quiescence and progression through G1 by phosphorylation of several transcriptional regulators, in particular the retinoblastoma protein family members (p107, p130, pRb), together with CDK6.[11] This phosphorylation further induces the de-repression of E2F transcription factors, allowing the transcription of genes required for G1/S transition. Hyperactivation of CDK4/cyclin D1 associated with genetic mutation, amplification or overexpression of either subunit has been widely documented in a great variety of human cancers, including breast cancer, neuroblastoma, mantle cell lymphoma and multiple myelomas, melanoma and lung cancers, contributing to enhancing and sustaining cancer cell proliferation.[8b] This kinase has thus been identified as a relevant target for anticancer therapeutics.[12]

The crystal structures of CDK4/cyclin D1 and CDK4/cyclin D3 suggest that these complexes adopt an "open conformation", with the interaction between CDK4 and its regulatory cyclin subunit appearing to be essentially mediated by the C helix (PISTVRE) of CDK4 and the α5 helix of the D-cyclin, in contrast to the "closed conformation" of CDK2/cyclin A (Figure 1).[13] However, a recent study addressing the conformational dynamics of CDK4/cyclin D inferred that this complex could adopt a conformation resembling that of CDK2/cyclin A.[14]

In this study we have chosen to investigate the utility of the two-branch anionic dye, TP-2Rho, to characterize peptide–protein and protein–protein interactions between the catalytic cyclin-dependent kinase CDK4 and its regulatory partner cyclin D1, and to compare the affinities of monomeric CDK4 and of the CDK4/cyclin D1 complex towards a peptide derived from retinoblastoma (Rb) substrate. Specifically, we report on the conjugation of TP-2Rho to the catalytic subunit of the CDK4, to a peptide derived from the main interface of CDK4 with cyclin D1, and to the Rb peptide, and their comparative titration against cyclin D1 protein, a peptide derived from the main interface of cyclin D1 with CDK4, and CDK4 monomer or CDK4/cyclin D heterodimer, respectively. We show that this dye is a much more sensitive probe for monitoring these peptide–protein and protein–protein interactions than other standard dyes. Finally we show that a TP-2Rho-conjugated peptide derived from CDK4 can be efficiently internalized into living cultured cells and provides a means of localizing endogenous CDK4/cyclin D.

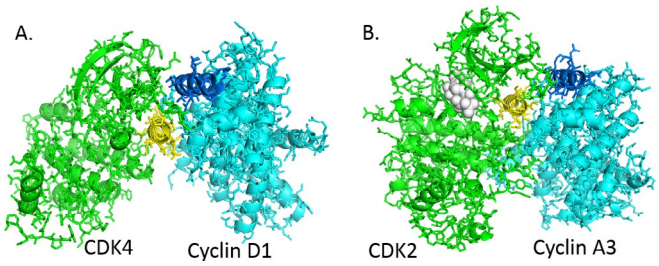

Figure 1. CDK4/cyclin D1 and CDK2/cyclin A. A) Stick representation of the "open conformation" of the crystal structure of CDK4/CycD1 (PDB 2W9F), the major interface between CDK4 (green) and cyclin D1 (cyan), consisting of the C helix (PISTVRE) and the α5 helix of cyclin D1, highlighted in yellow and dark blue, respectively. B) Stick representation of the "closed conformation" of the crystal structure of CDK2/cyclin A3 (PDB 1FIN), with the interface between CDK2 (green) and cyclin A3 (cyan) mediated by contacts between the C helix (PSTAIRE)/α5 helix of cyclin A3, highlighted in yellow and dark blue, respectively, as well as by additional contacts in the C lobe of CDK2.

Results and Discussion

Synthesis of the TP-2Rho-maleimide reagent

We chose to label peptides and proteins of interest on unique cysteine residues with a maleimide-conjugated derivative of TP-2Rho. We designed our conjugated compound with a C4 spacer. The TP-2Rho maleimide reagent (TP-2Rho-Mal) was prepared in six steps from (4-methoxyphenyl)diphenylamine (Scheme 1). Vilsmeier–Haack formylation followed by the deprotection of the phenolic function led to compound **3** in very good yields. The nucleophilic substitution of 1,4-dibromobutane by phenol **3** afforded the dialdehyde **4**. A furan-protected maleimide (to prevent maleimide polymerization) group was introduced through a nucleophilic substitution on bromide **4**. Compound **5** was deprotected (retro-Diels–Alder) without further characterization, and dialdehyde **6** was obtained in a very good yield. The last step was a Knoevenagel reaction on both aldehyde groups to provide TP-2Rho-Mal.

Photophysical properties of TP-2Rho-Mal

The photophysical properties of this compound were studied in PBS buffer and in glycerol (Table 1) and compared with those of TP-2Rho. As expected of the TP-Rho series, the compound was poorly fluorescent in aqueous medium (Figure 2). In glycerol, however, both TP-2Rho-Mal and TP-2Rho are fluorescent, displaying yellow emission with good quantum yields

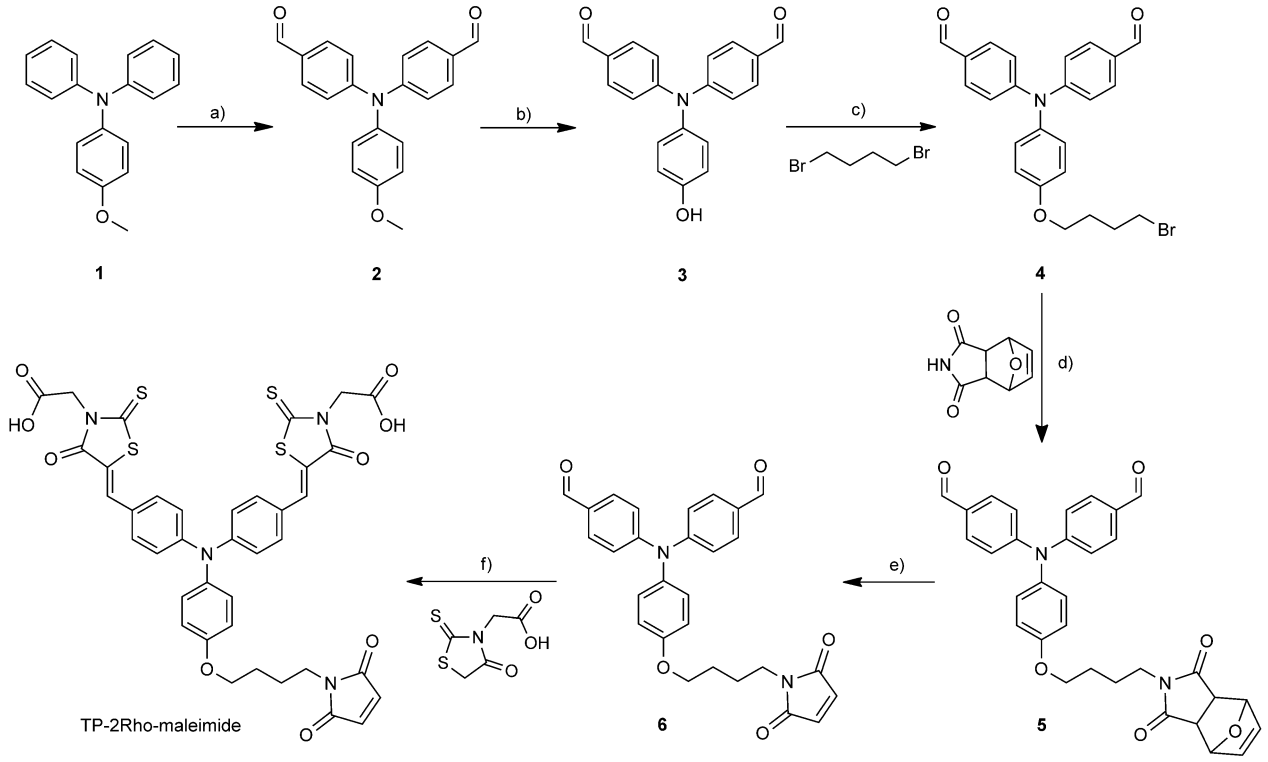

Scheme 1. Synthesis of TP-2Rho-Mal. a) $POCl_3$, DMF (78%); b) BBr_3, CH_2Cl_2 (92%); c) Cs_2CO_3, DMF (41%); d) K_2CO_3, DMF, 40 °C, 15 h (63%); e) toluene, reflux, 12 h (95%); f) NH_4OAc, H_3COOH, 115 °C, 16 h (35%).

Table 1. Photophysical properties of TP-2Rho-Mal and TP-2Rho.

Compounds	ε [mol^{-1} L cm^{-1}]		$\lambda_{abs}/\lambda_{em}$		Φ_F	
	PBS	glycerol	PBS	glycerol	PBS	glycerol
TP-2Rho-Mal	42000	52000	505/650	513/618	<0.005	0.04
TP-2Rho	53500	76300	505/633	500/615	<0.005	0.09

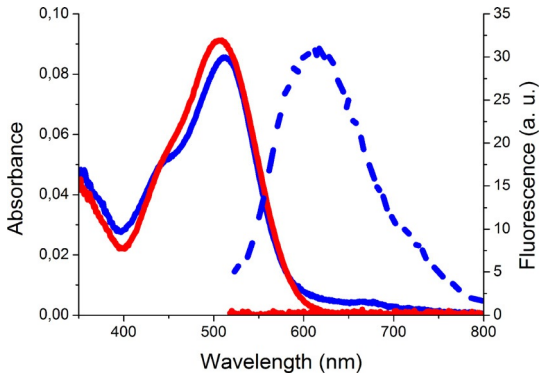

Figure 2. Absorption (——) and emission (····) spectra of 2 μM TP-2Rho-Mal in PBS buffer in red ($\lambda_{abs/em\,max}$: 505/650 nm; note that 30 μM was used to determine emission spectrum in PBS) and in glycerol in blue ($\lambda_{abs/em\,max}$: 513/618 nm).

from 0.04 to 0.09. This behaviour means that our probe is responsive to the constraints of environment, glycerol being a viscous solvent commonly used to restore fluorescence through restriction of molecular motions. The same fluorescence restoration can be expected for our probes (in monitoring of protein–protein interactions), because immobilization in glycerol can mimic the confinement of the probe between two peptide or protein partners. Both dyes display very large Stokes shifts (from 100 to 150 nm) in buffer and in glycerol.

Peptide–peptide interactions

In order to determine whether the TP-2Rho probe could be used to characterize the interaction between the C helix (PISTVRE) of CDK4 and the α5 helix of cyclin D1, we labelled a peptide derived from the PISTVRE helix (PISTVRE peptide) with this probe and titrated it against increasing concentrations of a peptide derived from the α-helix of cyclin D1 (α5 D1 peptide). For comparison we also labelled the PISTVRE peptide with other traditional probes, including FITC, BODIPY, coumarin, rhodamine, Cy3 and Cy5. As shown in Figure 3, TP-2Rho exhibited a tenfold increase in fluorescence upon titration with the α5 D1 peptide, whereas the other probes exhibited much lower fluorescence enhancement. Moreover, curve fitting and calculation of the dissociation constants revealed essentially similar values when titration was performed with TP-2Rho-, FITC- or BODIPY-labelled PISTVRE peptide of 11–12 μM, and a somewhat lower affinity for the Cy5-labelled peptide, with a dissociation constant value of (23±13) μM (Table 2). Moreover, upon interaction with α5 D1 peptide, we observed a shift of the PISTVRE-labelled TP-2Rho fluorescence maximum emission from 616 to 608 nm (Figure 3C).

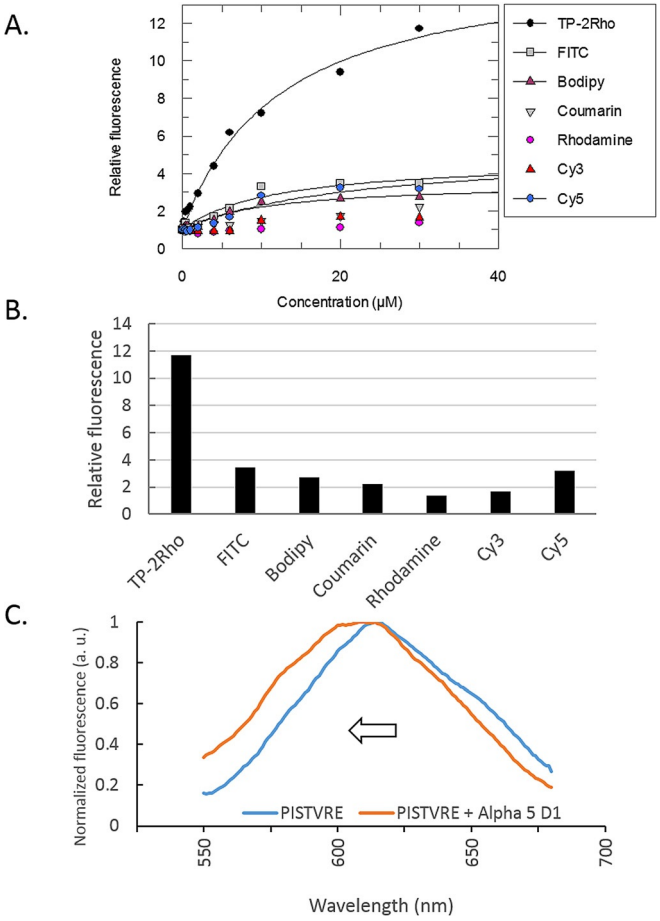

Figure 3. Titration of the fluorescently labelled PISTVRE peptide against α5 D1 peptide. A) Titration of PISTVRE labelled variously with TP-2Rho (200 nM, λ_{ex} = 510 nm, λ_{em} = 614 nm), FITC (200 nM, λ_{ex} = 483 nm, λ_{em} = 530 nm), BODIPY (200 nM, λ_{ex} = 477 nm, λ_{em} = 525 nm), coumarin (200 nM, λ_{ex} = 398 nm, λ_{em} = 484 nm), rhodamine (200 nM, λ_{ex} = 550 nm, λ_{em} = 605 nm), Cy3 (200 nM, λ_{ex} = 530 nm, λ_{em} = 580 nm) or Cy5 (200 nM, λ_{ex} = 610 nm, λ_{em} = 675 nm) against α5 D1 peptide. B) Histogram representation of maximum fluorescence enhancement upon titration against 30 μM α5 D1 peptide. C) Normalized fluorescence spectrum of TP-2Rho-labelled PISTVRE peptide before (blue) and after (red) incubation with αD1 peptide.

Table 2. Dissociation constants calculated for interaction between PISTVRE and α5 D1 peptides.

Labelled peptide	K_d [μM]	Labelled peptide	K_d [μM]
PISTVRE-TP-2Rho	12 ± 2	PISTVRE-rhodamine	–
PISTVRE-FITC	12 ± 5	PISTVRE-Cy3	–
PISTVRE-BODIPY	11 ± 4	PISTVRE-Cy5	23 ± 13
PISTVRE-coumarin	–		

Taken together, these data indicate that TP-2Rho is a highly sensitive probe for monitoring the interaction between two peptides, in comparison with other frequently used dyes such as FITC, BODIPY, coumarin, rhodamine, Cy3 and Cy5. Moreover TP-2Rho does not affect the interaction between two peptides derived from the natural occurring primary protein–protein interface of CDK4/cyclin D any more than FITC or BODIPY. This having been said, the micromolar affinities of the interaction between these peptides and the lower (by twofold) dissociation constant determined for the Cy5-PISTVRE/D1 peptide suggest that TP-2Rho, FITC and BODIPY might contribute to promoting the interaction between two peptides that exhibit a natural tendency to interact when surrounded by their complete protein environments but are less prone to interact in an unstructured form in solution.

Peptide–protein interactions

We next asked whether TP-2Rho could similarly serve to report on the interaction between the PISTVRE helix-derived peptide of CDK4 and cyclin D1. As shown in Figure 4A, titration of the TP-2Rho-labelled-PISTVRE peptide with glutathione *S*-transferase (GST)-cyclin D1 yielded a 19-fold increase in fluorescence emission intensity of this probe, with a K_d value of (351 ± 94) nM. In comparison, the TAMRA-labelled PISTVRE only yielded a three- to fourfold increase in fluorescence enhancement at saturation, with a K_d value of (152 ± 51) nM. As in the case of the peptide–peptide experiments, these results reveal that TP-2Rho is a highly sensitive probe for monitoring interactions between peptides and proteins. Moreover, titration experiments show that the PISTVRE helix of CDK4 interacts with 34-fold tighter affinity with cyclin D1 than with the α5 helix alone. This finding is in agreement with structural data that show how the PISTVRE helix interacts with an overall broader surface of cyclin D1 rather than just with the residues of the α5 helix (i.e., that the residues of the PISTVRE helix "sit within a pocket" of cyclin D1; Figure 4B, C). The difference in dissociation constant values determined for this interaction with TP-2Rho- or

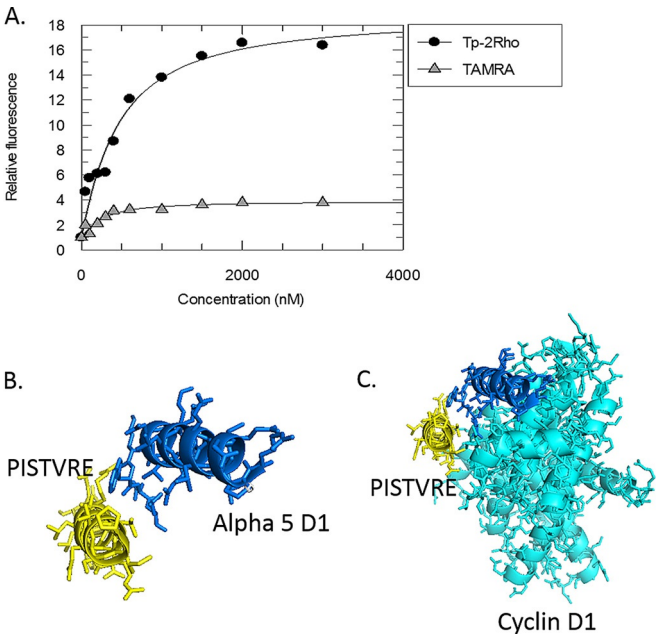

Figure 4. A) Titration of PISTVRE peptide labelled either with TP-2Rho (200 nM, λ_{ex} = 510 nm, λ_{em} = 614 nm) or with TAMRA (200 nM, λ_{ex} = 535 nm, λ_{em} = 585 nm) against GST-cyclin D1. B) Stick/surface representation of the PISTVRE peptide (yellow)/α5 D1 peptide (blue) interaction. C) Stick/surface representation of the PISTVRE peptide (yellow)/cyclin D1 protein (cyan) interaction.

TAMRA-labelled peptide is indicative of different contributions of these dyes to stabilizing the interaction. Nevertheless, these values are within the same sub-micromolar range, and not considerably different from those determined in the peptide/peptide titration experiments described above.

To investigate the potential of TP-2Rho to monitor peptide–protein interactions further, we titrated a TP-2Rho-labelled peptide derived from the substrate of CDK4, retinoblastoma protein, with GST-CDK4 and with the GST-CDK4/cyclin D complex.

Figure 5 reveals a significantly greater affinity of the Rb substrate for the complex, with a dissociation constant of (50±9) nM, than for monomeric GST-CDK4, with a calculated dissociation constant of (1470±28) nM. Moreover, binding of CDK4/cyclin D1 to the Rb-labelled peptide induced a much greater

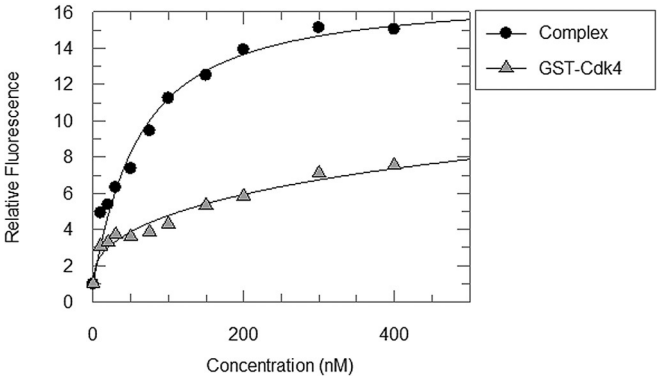

Figure 5. Titration of TP-2Rho-labelled (200 nM, $\lambda_{ex}=510$ nm, $\lambda_{em}=614$ nm) Rb substrate peptide against GST-CDK4 and against GST-CDK4/cyclin D1.

fluorescence enhancement than monomeric CDK4: 15-fold versus sixfold, respectively, at 400 nM. These findings are in line with previous studies that reported that CDK2/cyclin A has a higher affinity than monomeric CDK2 for its histone substrate, because the cyclin promotes a significant conformational change of CDK2, thereby favouring substrate binding in the catalytic cleft. However, it should be noted that the structure of monomeric CDK4 has not been solved, and that therefore there is no means of assessing whether cyclin D1 binding induces conformational reorganization of CDK4. Our results are therefore the first to indicate that this conformational change is likely to occur, because the Rb substrate binds CDK4/cyclin D1 with 30-fold greater affinity and a threefold greater fluorescence enhancement than monomeric CDK4.

Protein–protein interactions

We finally addressed whether TP-2Rho was applicable for monitoring of protein–protein interactions. To this end we labelled a mutant of GST-CDK4 that contains only two cysteine residues (C78 and C135, above and below the C α-helix) instead of four. This form of GST-CDK4 was labelled either with TP-2Rho or with Cy3 and titrated against cyclin D1 (Figure 6). Once again, these experiments revealed that TP-2Rho was a more sensitive

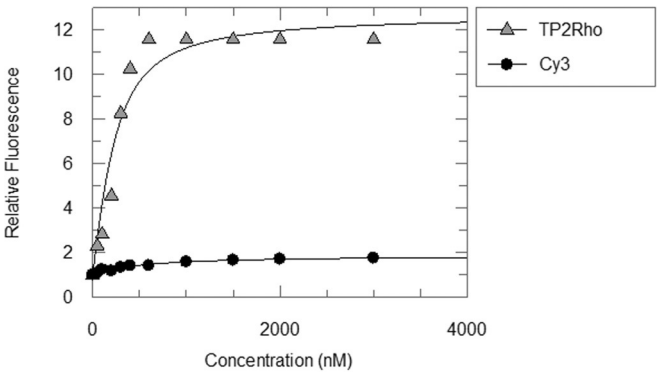

Figure 6. Titration of GST-CDK4 mutant (C78 C135) labelled either with TP-2Rho (200 nM, $\lambda_{ex}=510$ nm, $\lambda_{em}=614$ nm) or with Cy3 (200 nM, $\lambda_{ex}=530$ nm, $\lambda_{em}=580$ nm) against GST-cyclin D1.

probe than Cy3, because maximum fluorescence emission at saturation reached 13-fold with TP-2Rho, in comparison with twofold with Cy3. Titration of TP-2Rho-labelled GST-CDK4 mutant with GST-cyclin D1 yielded a K_d value of (123±47) nM. A somewhat greater K_d value of (445±88) nM was calculated for the interaction between the Cy3-labelled GST-CDK4 mutant and GST-cyclin D1. This finding suggests either that TP-2Rho might be contributing to the interaction, or that Cy3 might somehow be preventing efficient interactions. Nonetheless, these values are within the same sub-micromolar range indicative of an interaction between CDK4 and cyclin D1 that is 50–100 times tighter than that between the individual peptides derived from the PISTVRE helix of CDK4 and the α5 helix of cyclin D1.

TP-2Rho-labelled PISTVRE peptide colocalizes with intracellular target proteins

Finally, we speculated as to whether TP-2Rho might, when conjugated to the PISTVRE peptide, serve as a probe to colocalize endogenous cyclin D1 in HeLa cells. As expected, the PISTVRE-TP-2Rho-labelled peptide did not enter cells. We therefore used a Pep-PISTVRE peptide, which bears an N-terminal fusion of the Pep1 cell-penetrating peptide[15] to the sequence of PISTVRE, and found that it penetrated readily both into the cytoplasm and into the nucleus when overlaid onto HeLa cells (Figure 7A). To address the issue of whether this peptide indeed colocalized with cyclin D1 and CDK4, we performed indirect immunofluorescence on HeLa cells overlaid with the TP-2Rho-labelled Pep-PISTVRE peptide (Figure 7B). These experiments revealed a significant overlay of the TP-2Rho signal and of the signal revealed with Alexa647-labelled secondary antibodies against the rabbit polyclonal anti-CDK4 or anti-cyclin D1 antibodies.

Conclusions

Although small-molecule fluorescent probes offer the promise of monitoring peptide–peptide and protein–protein interactions,[16] they are not always suited to respond in a robust,

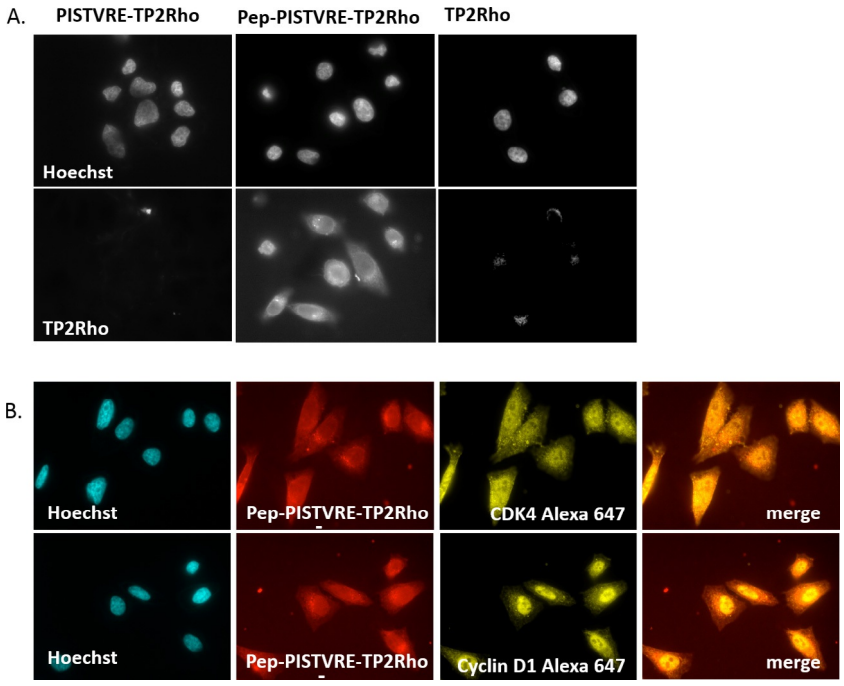

Figure 7. TP-2Rho-labelled Pep-PISTVRE peptide penetrates into HeLa cells and colocalizes with intracellular CDK4/cyclin D1 in HeLa cells. A) TP-2Rho Pep-PISTVRE peptide (2 μM) was found, on imaging with Cy3 filters, to have readily penetrated HeLa cells (centre), whereas the TP-2Rho-labelled PISTVRE peptide (left) and TP-2Rho (right) had not. Nuclear staining with Hoechst 33342 is shown in the upper panels, whereas the lower panels represent fluorescence emission of TP-2Rho with use of the Cy3 filter of the microscope. B) Anti-CDK4 and anti-cyclin D1 immunofluorescence performed on HeLa cells overlaid with 2 μM TP-2Rho Pep-PISTVRE peptide. Upper panels show the colocalization of the TP-2Rho-labelled Pep-PISTVRE peptide with CDK4. Lower panels show its co-localization with cyclin D1. Anti-CDK4 and anti-cyclin D1 immunostainings were revealed with Alexa647 secondary antibodies.

sensitive fashion. Moreover, traditional fluorescent probes are based on modular core dyes that in some cases respond to environmental changes, yet do not exhibit significant on/off responses.[17] More recent developments in the chemistry of small-molecule fluorescent probes have yielded compounds that are essentially dark prior to conjugation or binding to protein/peptide scaffolds.[18] Such dyes make highly sensitive probes for studies directed towards dissecting interactions between peptides and proteins and requiring selective tools to quantify, to compare and to highlight differences in affinity and specificity.

Here we have described the synthesis and conjugation of a switchable fluorescent vinyltriphenylamine dye, TP-2Rho, in order to characterize the mechanism of interaction between the catalytic kinase subunit CDK4 and its regulatory subunit cyclin D1, using peptide and protein derivatives of this heterodimeric kinase as well as a peptide substrate derived from Rb. Throughout this study we have clearly demonstrated that TP-2Rho is a superior dye, in terms of sensitivity, to other dyes traditionally used for monitoring peptide–protein and protein–protein interactions. Moreover, our results provide new information, complementary to structural studies on this heterodimeric complex, relating to the interactions that mediate assembly of CDK4/cyclin D1 and its ability to bind its substrate. Titration of the TP-2Rho-labelled-PISTVRE peptide with the complementary peptide interface of cyclin D1 yielded a dissociation constant of 12 μM and 15-fold increase in fluorescence. In comparison, titration of this same peptide with GST-cyclin D1 yielded an 18-fold increase in fluorescence emission intensity of this probe, with a K_d value of (351 ± 94) nM, indicating that the surface provided by cyclin D1 protein offers a broader surface of interaction with the PISTVRE peptide than the α5 D1 peptide. A third titration experiment performed with a GST-CDK4 protein bearing two TP-2Rho probes labelled above and below the PISTVRE helix and GST-cyclin D1 yielded a K_d value of (123 ± 47) nM with a 13-fold increase in fluorescence. This again reveals a tighter interaction between CDK4 and cyclin D1.

Furthermore, because there is no structural information available for monomeric CDK4, it is difficult to identify any conformational changes that might arise upon its interaction with cyclin D1. Nevertheless, these changes can be inferred from the major differences in fluorescence enhancement of the TP-2Rho probe conjugated to a substrate peptide, associated with a net increase in its affinity for CDK4/cyclin D1 relative to monomeric CDK4, emphasizing the utility of the highly sensitive TP-2Rho probe in dissection of the intricate steps of protein kinase regulation through assembly of a catalytic and regulatory subunit.

Finally, we have successfully employed TP-2Rho-labelled peptides to probe endogenous CDK4/cyclin D1 in living cells, indicating the potential of TP-2Rho for cellular imaging applications.

Experimental Section

General: All chemicals were purchased from Sigma–Aldrich or Acros Organics and were used as received. All other chemicals were used as received from the appropriate suppliers. Preparative flash chromatography was carried out with Merck silica gel (Si 60, 35–70 μm). NMR spectra were recorded with a Bruker Advance 300 spectrometer; ^{1}H NMR spectra were recorded at 300 MHz and ^{13}C NMR spectra at 75 MHz. Chemical shifts are reported in ppm downfield from TMS ($\delta = 0.00$) for ^{1}H NMR and from the central $CDCl_3$ resonance ($\delta = 77.16$) or [D_6]DMSO resonance ($\delta = 39.52$) for ^{13}C NMR. HPLC was carried out with a Waters Alliance instrument equipped with a photodiode array detector and a Xterra MS column with a linear gradient of acetonitrile versus water containing 0.1% FA ranging from 10 to 55% over 5 min and then to 100% over 6 min at a flow rate of 1 mL min^{-1}. Mass spectrometry was performed at the Institut Curie for Electrospray Ionization (ESI). HRMS was performed at the Institut de Chimie des Substances Naturelles (ICSN) in Gif-sur-Yvette.

4,4′-Bisformyl-4″-methoxytriphenylamine (2): $POCl_3$ (10 mL, 16.7 g, 109 mmol, 15 equiv) was added dropwise, at 0 °C under Ar, over 15 min to DMF (9 mL, 7.9 g, 109 mmol, 15 equiv). The solution was stirred at 0 °C for 1 h. 4-Methoxytriphenylamine (2 g, 7.26 mmol) was added, and the solution was stirred at 95 °C for 4 h 30 min. The dark mixture was poured into an ice bath and stirred for 30 min. The solution was basified with NaOH (1 M). The aqueous phase was extracted with CH_2Cl_2, and the organic phase was washed twice with water, dried over $MgSO_4$ and concentrated under reduced pressure to give a black oil. Purification by flash chromatography using CombiFlash (AcOEt/cyclohexane 10:80 to 70:30) afforded the title compound (1.72 g, 5.19 mmol, 71%). CAS number [149676-16-4]; ^{1}H NMR (300 MHz, $CDCl_3$): $\delta = 9.87$ (s, 2H), 7.75 (d, $J = 9$ Hz, 4H), 7.16 (d, $J = 9$ Hz, 4H), 7.11 (d, $J = 9.0$ Hz, 2H), 6.94 (d, $J = 9.0$ Hz, 2H), 3.84 ppm (s, 3H).

4,4′-Bisformyl-4″-hydroxytriphenylamine (3): BBr_3 (2.7 mL, 7.21 g, 28.79 mmol, 3 equiv) was added dropwise at 0 °C to a solution of **2** (3.18 g, 9.6 mmol, 1 equiv) in CH_2Cl_2 (20 mL). The reaction mixture was then allowed to warm slowly to RT and stirred for 3 h. The solution turned from yellow to dark. The mixture was then slowly poured into an ice bath. The aqueous phase was extracted twice with CH_2Cl_2. The combined organic phases were washed twice with water, dried over $MgSO_4$ and concentrated to give a green foamy solid. Purification by flash chromatography using CombiFlash (AcOEt/cyclohexane 10:90→60:40) afforded the title compound (2.8 g, 8.82 mmol, 92%) as a yellow solid. CAS number [336619-78-4]; ^{1}H NMR (300 MHz, $CDCl_3$): $\delta = 9.88$ (s, 2H), 7.76 (d, $J = 8.5$ Hz, 4H), 7.17 (d, $J = 8.5$ Hz, 4H), 7.07 (d, $J = 8.5$ Hz, 2H), 6.89 ppm (d, $J = 8.5$ Hz, 2H).

4′,4″-Bisformyl-4-(4-bromobutoxy)triphenylamine (4): A solution of caesium carbonate (4.1 g, 12.6 mmol, 5 equiv) and **3** (0.8 g, 2.52 mmol, 1 equiv) in anhydrous DMF (30 mL) was stirred at room temperature for 15 min. 1,4-Dibromobutane (4.5 mL, 37.5 mmol, 15 equiv) was then added, and the resulting mixture was stirred at room temperature for 2 h. The reaction mixture was then concentrated under reduced pressure. Water (20 mL) was added to the residue, and the obtained aqueous phase was extracted twice with CH_2Cl_2. The organic phase was washed twice with water, dried over $MgSO_4$ and concentrated to give a yellow oil. Purification by flash chromatography using CombiFlash (AcOEt/cyclohexane 10:90 to 60:40) afforded the title compound (475 mg, 1.05 mmol, 42%) as a yellow oil. ^{1}H NMR (300 MHz, $CDCl_3$): $\delta = 9.88$ (s, 2H), 7.76 (d, $J = 8.5$ Hz, 4H), 7.16 (d, $J = 8.5$ Hz, 4H), 7.11 (d, $J = 9$ Hz, 2H), 6.92 (d, $J = 9$ Hz, 2H), 4.02 (t, $J = 6$ Hz, 2H), 3.51 (t, $J = 6.5$ Hz, 2H), 2.16–1.92 ppm (m, 4H); ^{13}C NMR (75 MHz, $CDCl_3$): $\delta = 190.62$, 157.58, 152.21, 138.23, 131.41, 131.06, 129.03, 122.18, 116.09, 67.30, 33.47, 29.55, 27.99 ppm; MS (ES+): *m/z*: 453.0.

4′,4″-Bisformyl-4-(4-maleimidobutoxy)triphenylamine (6): 3a,4,7,7a-Tetrahydro-2*H*-4,7-epoxyisoindole-1,3-dione ([6253–28–7], 487 mg, 2.95 mmol, 2 equiv) and potassium carbonate (407 mg, 2.95 mmol, 2 equiv) were added under argon to a solution of dialdehyde **4** (667 mg, 1.47 mmol, 1 equiv) in anhydrous DMF (40 mL). The resulting mixture was stirred for one hour at room temperature and overnight at 40 °C. Solvents were removed under reduced pressure. Water (20 mL) was added to the residue, and the obtained aqueous phase was extracted twice with CH_2Cl_2. The organic phase was washed twice with water, dried over $MgSO_4$ and concentrated. After inspection by LC-MS, the protected maleimide **5** was dissolved in toluene (50 mL) and stirred at 120 °C overnight. After concentration, purification by flash chromatography using CombiFlash (CH_2Cl_2/EtOH 100 to 98:2) afforded the title compound (354 mg, 0.75 mmol, 51%) as a yellow oil. ^{1}H NMR (300 MHz, $CDCl_3$): $\delta = 9.87$ (s, 2H), 7.75 (d, $J = 8.5$ Hz, 4H), 7.15 (d, $J = 8.5$ Hz, 4H), 7.09 (d, $J = 9$ Hz, 2H), 6.91 (d, $J = 9$ Hz, 2H), 6.71 (s, 2H), 3.99 (m, 2H), 3.61 (m, 2H), 1.80 ppm (m, 4H); ^{13}C NMR (75 MHz, $CDCl_3$): $\delta = 190.66$, 170.98, 157.61, 152.22, 138.15, 134.26, 131.42, 131.02, 129.02, 122.17, 116.12, 67.53, 37.62, 26.60, 25.47 ppm; MS (ES$^+$): *m/z*: 469.2; HRMS (ESI$^+$): *m/z* calcd for $C_{28}H_{24}N_2O_5$: 469.1763; found 469.1768

TP-2Rho-maleimide: Dialdehyde **6** (180 mg, 0.38 mmol), rhodamine-3-acetic acid (162 mg, 0.84 mmol, 2.2 equiv) and ammonium acetate (119 mg, 1.53 mmol, 4 equiv) were dissolved in acetic acid (50 mL). The solution was stirred at 110 °C overnight. The reaction mixture was allowed to cool to room temperature and concentrated under vacuum until approximatively 10 mL of acetic acid remained. Ether was then added to the solution, and a dark red precipitate formed. The solid was filtered, washed with ether and dried to afford the expected product (142 mg, 0.17 mmol, 46%) as a dark red powder. M.p. 244–246 °C; ^{1}H NMR (300 MHz, DMSO): $\delta =$ 7.75 (s, 2H), 7.60 (d, $J = 9$ Hz, 4H), 7.14 (m, 6H), 7.01 (m, 4H), 4.54 (s, 4H), 4.00 (t, $J = 5$ Hz, 2H), 3.48 (t, $J = 6$ Hz, 2H), 1.72–1.64 ppm (m, 4H); ^{13}C NMR (75 MHz, DMSO): $\delta = 192.82$, 171.12, 167.16, 166.62, 157.04, 148.51, 137.33, 134.45, 132.79, 132.56, 128.93, 126.75, 122.20, 119.22, 116.08, 67.13, 46.27, 36.82, 25.98, 24.74 ppm; HRMS (ESI$^+$): *m/z* calcd for $C_{38}H_{30}N_4O_9S_4$: 815.0974; found 815.1003.

Peptide synthesis and labelling: Peptides used in this study were purchased from GL Biochem (Shanghai, P.R. China), labelled on their single cysteine residues with maleimide dye derivatives, in the presence of a five- to tenfold excess of dye overnight, and then purified from free dye on NAP-5 columns (GE Healthcare).

PISTVRE peptide: GGGCPISTVREVALLRRL

α5 D1 peptide: SIRPEELLQMELLLVNKLKWNLC

Rb peptide: YKFCSSPLRIPG

Pep-PISTVRE peptide: KETWWETWWTEKK GGGCPISTVREVALLRRL

Protein expression and purification of CDKs: Recombinant CDKs and cyclins were expressed in *Escherichia coli* by IPTG induction and purified by chromatography as described previously.[9h] GST-CDKs or cyclins were first purified on GSTTrap columns, followed by gel filtration chromatography on HiLoad 16/600 Superdex 75 preparatory grade.

Design and engineering of CDK4 mutant: The cDNA sequence of mouse CDK4 was cloned into the pGex6P1 vector (GE Healthcare)

5′-BamHI 3′-EcoRI. Cysteine residues 202 and 215 were mutagenized to serine, according to the QuickStart protocol (Stratagene), and DNA extracted from mutant *E. coli* colonies was sequenced to confirm mutations and to verify that no undesired mutations had occurred.

Fluorescence titration experiments: Fluorescence titration assays were performed in 96-well plates in potassium phosphate [200 μL, KH_2PO_4/K_2PO_4 (50 mM), pH 7.4] and NaCl (150 mM) solution with use of a Clariostar spectrofluorimeter (BMG). The fluorescently labelled peptides or proteins (200 nM) were excited at 510 nm, and emission signals were acquired at 614 nm unless stated otherwise. Data analysis was performed with the aid of the GraFit Software (Erithacus, Ltd., Horley, UK). Experiments were performed in triplicate, and error bars indicate standard deviations from averages.

Cell culture, internalization and microscopy: Cell culture media, serum and antibiotics were purchased from Invitrogen. HeLa cells were cultured in Dulbecco's modified Eagle's medium (DMEM) + Glutamax supplemented with foetal calf serum (FCS, 10%), penicillin G (sodium salt, 100 units mL^{-1}) and streptomycin (100 μg mL^{-1}) at 37 °C under an atmosphere containing CO_2 (5%).

TP-2Rho-labelled PISTVRE peptide or Pep-PISTVRE peptide (2 μM) was overlaid onto HeLa cells grown to 50–60% confluency for 1 h at 37 °C and then for another hour in the presence of DMEM complemented with serum (10%).

Cells were then fixed with formalin in phosphate-buffered saline (PBS) for 10 min and washed in PBS, and the nuclei were stained with Hoechst 33342. Indirect immunofluorescence was performed with rabbit polyclonal anti-CDK4 (C-22 from Santa Cruz) at 1:250 dilution or anti-cyclin D1 antibody (C-20 from Santa Cruz) at 1:250 dilution in blocking buffer [BSA (4%), goat serum (4%), Triton (0.1%)] overnight, washing, subsequent incubation with Alexa647-conjugated secondary antibodies at 1:500 dilution for 1 h, washing again in PBS, staining of nuclei with Hoechst 33342, washing in water and mounting on glass slides in Mowiol. Fluorescent cells were observed with a Zeiss microscope equipped with a CoolSnap camera and images were acquired with the aid of MetaMorph software. Excitation band/dichroic/emission band filters for imaging fluorescent signals were as follows: Hoechst 33342: 340–380/400/450–490 nm. Alexa647-conjugated antibodies were imaged by using the Cy5 filters: 590–650/660/662–737 nm. TP-2Rho fluorescence was imaged by using the Cy3 filters: 525–565/565/572–647 nm.

Acknowledgements

This work was supported by the CNRS (Centre National de la Recherche Scientifique) and a grant from the Institut de Recherche contre Cancer (INCA) to M.C.M. This work has benefited from the facilities and expertise of the Small Molecule Mass Spectrometry platform of IMAGIF (Centre de Recherche de Gif: www.imagif.cnrs.fr), and of the Montpellier RIO imaging facility (www.mri.cnrs.fr) at the Centre de Recherches en Biochimie Macromoléculaire, Montpellier.

Keywords: biosensors · CDK4/cyclin D kinase · peptide–peptide/protein interactions · protein–protein interactions · solvatochromic fluorescent probes

[1] X. Li, X. Gao, W. Shi, H. Ma, *Chem. Rev.* **2014**, *114*, 590 – 659.
[2] a) M. E. Vázquez, J. B. Blanco, B. Imperiali, *J. Am. Chem. Soc.* **2005**, *127*, 1300 – 1306; b) G. Loving, B. Imperiali, *J. Am. Chem. Soc.* **2008**, *130*, 13630 – 13638.
[3] a) I. A. Karpenko, M. Collot, L. Richert, C. Valencia, P. Villa, Y. Mely, M. Hibert, D. Bonnet, A. S. Klymchenko, *J. Am. Chem. Soc.* **2015**, *137*, 405 – 412; b) I. A. Karpenko, R. Kreder, C. Valencia, P. Villa, C. Mendre, B. Mouillac, Y. Mely, M. Hibert, D. Bonnet, A. S. Klymchenko, *ChemBioChem* **2014**, *15*, 359 – 363.
[4] a) C. Allain, F. Schmidt, R. Lartia, G. Bordeau, C. Fiorini-Debuisschert, F. Charra, P. Tauc, M. P. Teulade-Fichou, *ChemBioChem* **2007**, *8*, 424 – 433; b) B. Dumat, G. Bordeau, E. Faurel-Paul, F. Mahuteau-Betzer, N. Saettel, G. Metge, C. Fiorini-Debuisschert, F. Charra, M. P. Teulade-Fichou, *J. Am. Chem. Soc.* **2013**, *135*, 12697 – 12706.
[5] B. Dumat, G. Bordeau, A. I. Aranda, F. Mahuteau-Betzer, Y. El Harfouch, G. Metge, F. Charra, C. Fiorini-Debuisschert, M. P. Teulade-Fichou, *Org. Biomol. Chem.* **2012**, *10*, 6054 – 6061.
[6] a) W. R. Zipfel, R. M. Williams, W. W. Webb, *Nat. Biotechnol.* **2003**, *21*, 1369 – 1377; b) B. G. Wang, K. Konig, K. J. Halbhuber, *J. Microsc.* **2010**, *238*, 1 – 20.
[7] a) M. Malumbres, M. Barbacid, *Trends Biochem. Sci.* **2005**, *30*, 630 – 641; b) S. Lim, P. Kaldis, *Development* **2013**, *140*, 3079 – 3093.
[8] a) U. Asghar, A. K. Witkiewicz, N. C. Turner, E. S. Knudsen, *Nat. Rev. Drug Discovery* **2015**, *14*, 130 – 146; b) M. Peyressatre, C. Prével, M. Pellerano, M. Morris, *Cancers* **2015**, *7*, 179.
[9] a) D. O. Morgan, *Annu. Rev. Cell Dev. Biol.* **1997**, *13*, 261 – 291; b) A. J. Obaya, J. M. Sedivy, *Cell. Mol. Life Sci.* **2002**, *59*, 126 – 142; c) A. Satyanarayana, P. Kaldis, *Oncogene* **2009**, *28*, 2925 – 2939; d) P. D. Jeffrey, A. A. Russo, K. Polyak, E. Gibbs, J. Hurwitz, J. Massague, N. P. Pavletich, *Nature* **1995**, *376*, 313 – 320; e) A. A. Russo, P. D. Jeffrey, N. P. Pavletich, *Nat. Struct. Mol. Biol.* **1996**, *3*, 696 – 700; f) N. R. Brown, M. E. M. Noble, A. M. Lawrie, M. C. Morris, P. Tunnah, G. Divita, L. N. Johnson, J. A. Endicott, *J. Biol. Chem.* **1999**, *274*, 8746 – 8756; g) F. Heitz, M. C. Morris, D. Fesquet, J. C. Cavadore, M. Doree, G. Divita, *Biochemistry* **1997**, *36*, 4995 – 5003; h) M. C. Morris, C. Gondeau, J. A. Tainer, G. B. Divita, *J. Biol. Chem.* **2002**, *277*, 23847 – 23853.
[10] H. L. De Bondt, J. Rosenblatt, J. Jancarik, H. D. Jones, D. O. Morgant, S.-H. Kim, *Nature* **1993**, *363*, 595 – 602.
[11] a) A. Ho, S. F. Dowdy, *Curr. Opin. Genet. Dev.* **2002**, *12*, 47 – 52; b) S. J. Baker, E. P. Reddy, *Genes Cancer* **2012**, *3*, 658 – 669.
[12] a) M. Malumbres, M. Barbacid, *Nat. Rev. Cancer* **2001**, *1*, 222 – 231; b) Y. Dobashi, A. Goto, M. Fukayama, A. Abe, A. Ooi, *Int. J. Cancer* **2004**, *110*, 532 – 541; c) O. Gautschi, D. Ratschiller, M. Gugger, D. C. Betticher, J. Heighway, *Lung Cancer* **2007**, *55*, 1 – 14; d) M. Puyol, A. Martin, P. Dubus, F. Mulero, P. Pizcueta, G. Khan, C. Guerra, D. Santamaria, M. Barbacid, *Cancer Cell* **2010**, *18*, 63 – 73; e) E. A. Musgrove, C. E. Caldon, J. Barraclough, A. Stone, R. L. Sutherland, *Nat. Rev. Cancer* **2011**, *11*, 558 – 572; f) K. E. Sheppard, G. A. McArthur, *Clin. Cancer Res.* **2013**, *19*, 5320 – 5328.
[13] a) P. J. Day, A. Cleasby, I. J. Tickle, M. O'Reilly, J. E. Coyle, F. P. Holding, R. L. McMenamin, J. Yon, R. Chopra, C. Lengauer, H. Jhoti, *Proc. Natl. Acad. Sci. USA* **2009**, *106*, 4166 – 4170; b) T. Takaki, A. Echalier, N. R. Brown, T. Hunt, J. A. Endicott, M. E. M. Noble, *Proc. Natl. Acad. Sci. USA* **2009**, *106*, 4171 – 4176.
[14] N. Floquet, M. G. S. Costa, P. R. Batista, P. Renault, P. M. Bisch, F. Raussin, J. Martinez, M. C. Morris, D. Perahia, *Biophys. J.* **2015**, *109*, 1179 – 1189.
[15] M. C. Morris, J. Depollier, J. Mery, F. Heitz, G. Divita, *Nat. Biotechnol.* **2001**, *19*, 1173 – 1176.
[16] A. Hawe, M. Sutter, W. Jiskoot, *Pharm. Res.* **2008**, *25*, 1487 – 1499.
[17] L. D. Lavis, R. T. Raines, *ACS Chem. Biol.* **2008**, *3*, 142 – 155.
[18] a) M. P. Bruchez, *Curr. Opin. Chem. Biol.* **2015**, *27*, 18 – 23; b) L. M. Wysocki, L. D. Lavis, *Curr. Opin. Chem. Biol.* **2011**, *15*, 752 – 759; c) L. D. Lavis, R. T. Raines, *ACS Chem. Biol.* **2014**, *9*, 855 – 866.

Manuscript received: November 26, 2015
Accepted article published: March 4, 2016
Final article published: March 17, 2016